

Investigation of multi-phase erosion using reconstructed shale trends based on sonic data. Sole Pit axis, North Sea

Peter Japsen*

Geological Survey of Denmark and Greenland (GEUS), Thoravej 8, DK-2400 Copenhagen NV, Denmark

Received 8 November 1999

Abstract

Estimates from sonic data of removed overburden (burial anomalies) rely on identification of normal velocity–depth trends for relatively homogenous lithological units. In the North Sea, such trends are difficult to establish for Mesozoic formations that rarely are found at maximum burial and hydrostatic pressure. The analysis of erosional history based on sonic data can, however, be developed further where two homogeneous units are encountered in the same wells, because the two units may or may not have been simultaneously at maximum burial at a given location. If the two units were at maximum burial depth simultaneously prior to the most recent erosional event, the burial anomalies for the two units should be identical. If, however, the lower unit was at maximum burial before the upper unit, due to an intervening erosional event, the burial anomaly for the lower unit should exceed that of the upper unit.

In the North Sea, Neogene erosion can be estimated from burial anomalies for the Upper Cretaceous–Danian Chalk Group. This allows corrections to be made of the depths of pre-Chalk formations to the situation prior to the onset of Neogene erosion. The normal trend for the pre-Chalk formation can now be traced more easily in a plot of velocity versus corrected depth, because the pre-Chalk formation was at maximum burial at more locations prior to Neogene erosion. This procedure is used to derive baselines for a Lower Jurassic shale unit, and for the Lower Triassic Bunter Shale and Bunter Sandstone using data from 123 British and Danish wells. The dominance of smectite/illite in the marine Lower Jurassic shale, and of kaolin in the continental Bunter Shale may explain why these two baselines diverge, and why those for the Bunter Shale and Bunter Sandstone converge.

Burial anomalies for the Chalk Group and the Bunter Shale/Sandstone are calculated for 210 wells in the southwestern North Sea. Of these wells, 81 have data for both the Chalk and the Triassic level. The burial anomaly for the Triassic level exceeds that for the Chalk only along the Sole Pit axis. There, the Triassic deposits are suggested to have experienced maximum burial prior to an erosion event, in probably the Late Cretaceous or locally in the latest Jurassic. The erosion removed more than 2 km of mainly Jurassic–Lower Cretaceous or locally Triassic–Jurassic sediments. The burial anomalies for the Chalk and the Bunter levels are about identical over the rest of the southwestern North Sea Basin where they were both at maximum burial prior to Neogene erosion of up to 1 km of sediments of mainly Cenozoic age. © 2000 Elsevier Science B.V. All rights reserved.

Keywords: uplifts; velocity; burial depth; North Sea; Mesozoic; Cenozoic

1. Introduction

Sediment compaction studies based on sonic data are powerful methods for estimating maximum burial

* Fax: +45-38-14-20-50.

E-mail address: pj@geus.dk (P. Japsen).

depth of homogeneous lithological units. Measured velocity anomalies — or burial anomalies (Japsen, 1998) — relative to the normal velocity–depth trend for a lithological unit may be interpreted to be caused by a reduction of the overburden thickness (Fig. 1A). Velocity–depth data are easily available from numerous wells in basins throughout the world, and have thus been included in several studies of exhumation in recent years (e.g. Chadwick et al., 1994; Hillis, 1995; Hansen, 1996; Heasler and Kharitonova, 1996; Evans, 1997; Japsen, 1998).

However, the basis of the method is the derivation of normal velocity–depth trends (or baselines) that are geologically and physically constrained. Principles for the construction of such baselines are often violated, and this may lead to erroneous results that typically underestimate erosion. First, the identification of the data that represent normal compaction may be difficult in areas such as the North Sea Basin where the margins of the basin have been eroded and the centre of the basin is characterised by overpressure (compare Japsen, 1998). Second, the gradient of

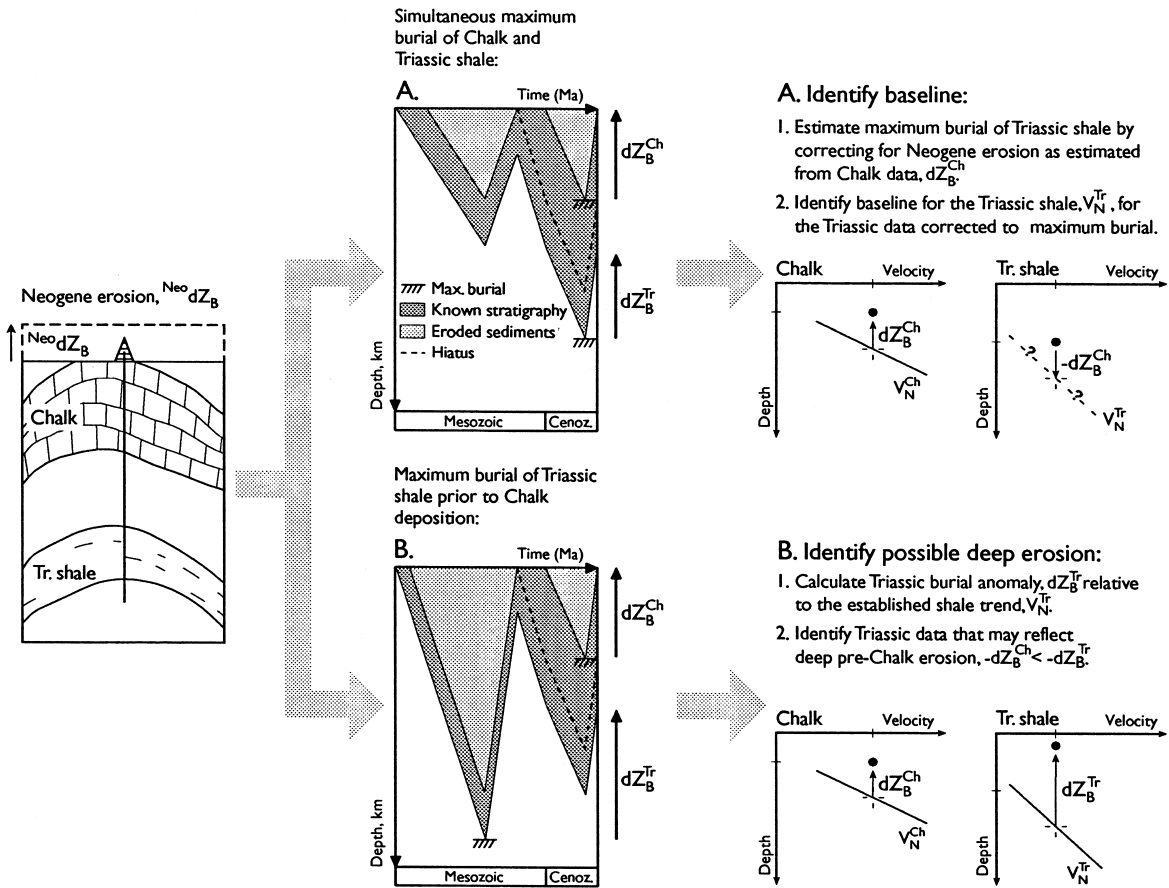


Fig. 1. Schematic burial diagrams for the Mesozoic succession illustrating the relationship between burial anomalies ('uplift') for the Chalk and the Triassic in the same well, dZ_B^{Ch} and dZ_B^{Tr} . Either the two units in the same well have been at maximum burial depth simultaneously or the lower unit has been at maximum burial prior to the upper unit due to an intervening erosional event. (A) The baseline for a Triassic formation, V_N^{Tr} , can be traced more easily if we correct the depth to the formation for the effect of Neogene erosion as estimated from the Chalk burial anomaly, dZ_B^{Ch} . (B) We can now calculate the burial anomaly for the Triassic formation, dZ_B^{Tr} , for all data points relative to V_N^{Tr} , and identify the wells where the magnitude of the Triassic anomaly exceeds that of the Chalk. These cases may reflect deep pre-Chalk erosion. Legend: \bullet , present-day velocity–depth data point; $+$, velocity–depth data point at time of maximum burial.

the velocity–depth function should approach zero at infinite depth (unlike, e.g. linear velocity–depth trends; see Appendix A). If it does not, too high normal velocities are predicted at depth, and this may lead to underestimates of the amount of erosion. Third, the shape of the baseline for a given rock type should reflect the physical properties of the rock and the reduction of porosity during normal burial. Identical mathematical formulations can thus not be expected to match the trends for different lithologies. Partly due to these problems, there is little agreement between the normal velocity–depth trends for the Mesozoic shale formations of the North Sea area presented by various workers (Jankowsky, 1962; John, 1975; Marie, 1975; Scherbaum, 1982; Bulat and Stoker, 1987; Hillis, 1995). The disagreements, however, also reflect major differences in the mineralogy of shale formation as it will be demonstrated here.

The analysis of the erosional history based on sonic data can be further refined in basins where two relatively homogeneous units have been penetrated in several wells. In this situation, only two very simple cases can occur. Either the two units in the same well have been at maximum burial depth simultaneously — in which case burial anomalies for the two units should be identical — or the lower unit has been at maximum burial prior to the upper unit due to an intervening erosional event — in which case the burial anomaly for the lower unit should exceed that for the upper unit (Fig. 1).

I apply this argument to the North Sea where the erosion of the basin margins during the Neogene can be estimated reliably from the burial anomaly of the Upper Cretaceous–Danian Chalk Group relative to its normal velocity–depth trend (Hillis, 1995; Japsen, 1998). It is thus possible to construct palaeo-velocity–depth plots for the situation prior to the Neogene erosion by correcting the present-day depths for pre-Chalk formations by the Chalk burial anomaly from the same well (Fig. 1). The normal velocity–depth trends for the pre-Chalk formation can now be identified more easily because that formation was at maximum burial at more locations prior to Neogene erosion than it is now. This procedure is used here to derive baselines for Lower Jurassic shale (the F-I Member of the Fjerritslev Formation) and for the Lower Triassic Bunter Shale and Sandstone using

interval velocity data from wells in Denmark and the UK southern North Sea (Fig. 2) (Bertelsen, 1980; Michelsen, 1989; Johnson et al., 1994).

Finally, I investigate data from the southwestern North Sea to try to differentiate those areas where maximum burial of the entire Mesozoic succession occurred during the Cenozoic, from areas of inversion along the Sole Pit axis where maximum burial of the Triassic deposits may have taken place during the Mesozoic. Previous studies have led to contradicting results concerning the effects of the erosional episodes in this area. (Marie, 1975; Glennie and Boegner, 1981; Bulat and Stoker, 1987; Hillis, 1995; Japsen, 1997, 1998).

2. Burial anomaly relative to a normal velocity–depth trend

A normal velocity–depth trend (baseline), $V_N(z)$, describes in a functional form how the sonic velocity of a relatively homogeneous sedimentary formation saturated with brine increases with depth during normal compaction (V is velocity [m/s], z is depth [m]). The pressure of the formation is hydrostatic during normal compaction, and the formation is at maximum burial depth; i.e. the thickness of the overburden has not been reduced by erosion. The identification of a baseline thus involves three steps of generalisation: identification of a relatively homogeneous lithological unit, selection of data points representing normal compaction, and finally, assigning a functional expression to the velocity–depth trend (e.g. Bulat and Stoker, 1987; Hillis, 1995; Japsen, 1998).

The burial anomaly, dZ_B [m], is the difference between the present-day burial depth of a rock, z , and the depth, $z_N(V)$, corresponding to normal compaction for the measured velocity, V :

$$dZ_B = z - z_N(V) \quad (1)$$

where $z_N(V)$ represents the inverted normal velocity–depth trend, $V_N(z)$, for the formation in question (Fig. 1; see list of symbols in Table 1) (Japsen, 1998). The burial anomaly is zero for normally compacted sediments, whereas high velocities rela-

Table 1
List of symbols

B_E	post-exhumational burial
V_N	normal velocity–depth trend for a given formation
V_0, V_∞	velocity at the surface and at infinite depth
$V_N^{BSh}, V_N^{Ch}, V_N^{LJur}$	normal velocity–depth trends for the Bunter Shale, the Chalk Group and the Lower Jurassic shale (Eqs. 5, B-1 and 4, respectively)
z	present-day burial depth of a rock
$z_{pre-Neo}$	estimate of formation depth prior to Neogene erosion (Eq. 3)
Δz_{miss}	missing overburden section removed by erosion (Eq. 2)
z_N	depth corresponding to normal compaction for measured V
dZ_B	burial anomaly relative to a normal velocity–depth trend (Eq. 1)
${}_{Neo}dZ_B, {}_{pre-Ch}dZ_B$	burial anomaly caused by Neogene or pre-Chalk erosion (see Fig. 7)
dZ_B^{BSh}, dZ_B^{BSs}	Bunter Shale and Bunter Sandstone burial anomaly relative to V_N^{BSh}
dZ_B^{Ch}	Chalk burial anomaly relative to V_N^{Ch}
dZ_B^{Tr}	Triassic burial anomaly from Bunter Shale and Sandstone data (see Section 3)
dZ_{p-B}^{Tr}	Triassic palaeo-burial-anomaly (= $dZ_B^{Tr} - dZ_B^{Ch}$)

tive to depth give negative burial anomalies which may be caused by a reduction in overburden thickness where the lithology is relatively homogenous over the study area, and if lateral variations in heat flow and horizontal stress are minor ('apparent uplift', Bulat and Stoker, 1987; 'net uplift and erosion', Riis and Jensen, 1992; 'apparent exhumation', Hillis, 1995). A positive burial anomaly may indicate undercompaction due to overpressure.

Whether a burial anomaly is a measure of erosion or is caused by other factors (e.g. lithological changes) need to be studied by an integrated evaluation of the area in question. Apart from matching other estimates of erosion, the burial anomalies should principally correspond geographically to where there is a missing section in the stratigraphic record. It must, however, be observed that any post-exhumational burial, B_E [m], will mask the magnitude of the missing overburden section, Δz_{miss} [m], and we get (Fig. 1, Table 1):

$$\Delta z_{miss} = -dZ_B + B_E, \quad (2)$$

where the minus indicates that erosion reduces depth (Hillis, 1995; Japsen, 1998). Knowledge of the timing of the erosional events thus becomes a critical aspect, not only for understanding the succession of events, but also for understanding their true magnitude, and for identifying the age of the eroded succession.

The increase of velocity with depth is often approximated by linear relationships between different

transformations of velocity and depth, but the most common expressions predict velocity to approach infinity with depth (see Appendix A for a more detailed discussion). The increase of velocity with depth should, however, approach zero. This constraint becomes important when considering depth intervals over several kilometres. Disregarding a proper mathematical formulation thus may lead to a severe underestimate of the amount of erosion because unconstrained trends predict too high velocities at depth. However, it must also be considered that the estimate of removed overburden becomes very sensitive to minor variations in velocity at great depth where a constrained baseline becomes ever steeper.

3. Data

The study is based on velocity–depth data from 210 wells in the UK southern North Sea and 51 Danish wells outside the late Cenozoic depocentre (Fig. 2). Velocity data for the UK wells were presented by Hillis (1995) and Japsen (1998), whereas the Danish wells were presented by Nielsen and Japsen (1991) (apart from the Jelling-1 well). Of the UK wells, 126 have measures of interval velocity for the Bunter Sandstone or Bunter Shale Formations, and 81 of these wells also have interval velocities from the Turonian–Maastrichtian Middle and Upper

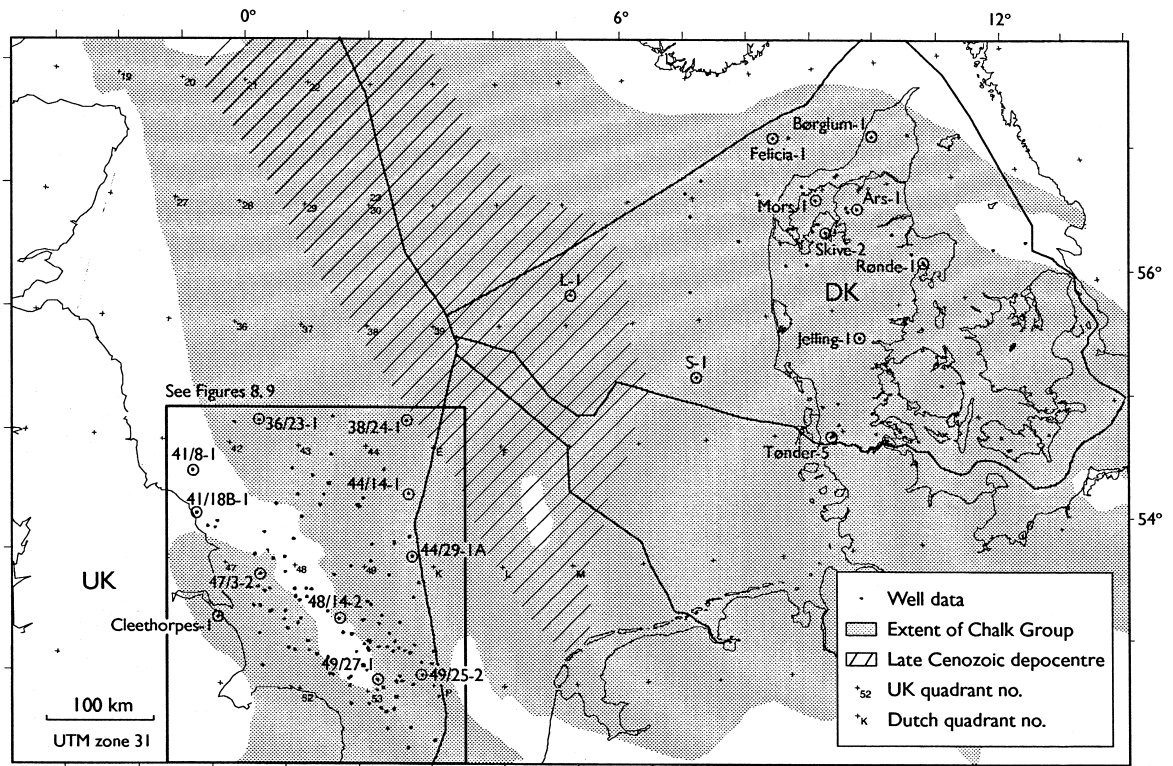


Fig. 2. Location of the wells studied with interval velocities for the Bunter Shale, Bunter Sandstone, or Lower Jurassic shale (F-1 Member of the Fjerritslev Formation). When Chalk velocity data are available for these wells, the Neogene erosion can be estimated and present burial depths for the pre-Chalk formations can be corrected for the effect of erosion. Outline of the late Cenozoic depocentre drawn where the thickness of these deposits exceeds 1.5 km.

Chalk (which constitutes the main part of the Chalk Group in the UK southern North Sea; Cameron et al., 1992). The rest of the UK wells just have velocity–depth data for the Chalk. The Danish wells have interval velocities from Lower Jurassic shale (the F-1 Member of the Fjerritslev Formation), from the Bunter Sandstone or the Bunter Shale, and 42 of these have data from the Chalk Group (cf. Japsen, 1993, 1998). A total of 99 wells have interval velocities for the Chalk and the Bunter Shale or Bunter Sandstone, and 27 wells for the Chalk and the F-1 Member. The overlap between these two groups consists of the Danish wells Felicia-1, Mors-1, and Rønde-1. Plots of interval velocities versus midpoint depth for the F-1 Member, the Bunter Shale and the Bunter Sandstone are shown in Figs. 3–5; the data points are plotted against both present-day depth, as well as depths corrected for Neogene erosion (Eq. 3).

Burial anomalies, dZ_B^{Ch} , dZ_B^{BSs} , and dZ_B^{BSH} , are calculated for the Chalk, the Bunter Sandstone, and the Bunter Shale (Table 2). Chalk burial anomalies are calculated relative to a revision of the baseline suggested by Japsen (1998) as described in Appendix B (Eq. B-1). The mean magnitude of 427 m for the estimated negative Chalk burial anomalies is about 200 m smaller than that estimated relative to the Chalk baselines of Hillis (1995) and Japsen (1998). The anomalies for both Triassic formations are calculated relative to the baseline for the Bunter Shale given by Eq. (5) (see below). A single, Triassic burial anomaly, dZ_B^{Tr} , is computed for each well. The value used is normally that from the Bunter Shale value (117 wells) because shale is considered to be more uniform than sandstone. However, to be conservative, the value from the Bunter Sandstone is used where the Shale value exceeds the Sandstone

Table 2

Burial anomalies for wells in the UK southern North Sea

Listing of burial anomalies for wells with velocity data for both the Chalk and the Bunter Sandstone or Bunter Shale, and for wells for which the magnitude of the Triassic burial anomaly exceeds 2 km. Only 10 out of 25 data points are shown for block 49. Based on interval velocity data given in Hillis (1995) (his table 2). List of mathematical symbols in Table 1.

Numbers in (), Triassic anomaly not used in contouring because $-dZ_{p-B}^{Tr} < 350$; Cleeth.: Cleethorpes-1.

Well symbols (compare Fig. 7): • Neogene erosion from mean anomaly from Chalk and Triassic data, Chalk anomaly weighted twice as the Triassic anomaly; ⊙ Neogene erosion from Chalk data, pre-Chalk erosion from Triassic data not used (in parentheses), magnitude of Triassic anomaly exceeds that of Chalk by 250–350 m; ⊖ Neogene erosion from Chalk data, pre-Chalk erosion from Triassic data, magnitude of Triassic anomaly exceeds that of Chalk by more than 350 m; □ Neogene erosion from Triassic data, Chalk data erroneous; ◇ Neogene erosion from Chalk data, Triassic data erroneous; △ Pre-Chalk erosion from Triassic data, no Chalk data, only mapped within contiguous area along Sole Pit axis; + Neogene erosion from Chalk data only (not listed in Table 1, but shown on Fig. 9).

Well		$-dZ_B^{Neo}$	$-dZ_B^{preCh}$	$-dZ_{p-B}^{Tr}$	$-dZ_B^{Ch}$	$-dZ_B^{Tr}$	$-dZ_B^{BSH}$	$-dZ_B^{BSs}$
36/23-1	•	606	–	9	603	612	612	–
36/26-1	•	1007	–	35	995	1030	1030	–
37/23-1	⊙	–125	(137)	262	–125	137	137	–
38/24-1	•	–205	–	55	–223	–169	–169	–
41/18B-1	△	–	2527	–	–	2527	3260	2527
41/20-2	△	–	2141	–	–	2141	2141	1757
41/24A-2	△	–	2273	–	–	2273	2716	2273
41/25A-1	△	–	2537	–	–	2537	2537	2239
42/10A-1	•	518	–	110	482	592	592	–
42/23-1	△	–	2636	–	–	2636	2636	4235
42/28-2	□	730	–	–362	1092	730	730	876
43/11-1	•	775	–	204	707	910	910	2059
43/12-1	⊙	484	802	318	484	802	802	1212
43/13A-1	⊖	372	741	369	372	741	741	461
43/15-1	□	244	–	–307	551	244	244	329
43/20-1	•	436	–	83	408	491	491	339
43/3-1	•	203	–	–97	236	138	138	857
43/30-1	•	677	–	231	599	831	831	899
43/7-1	•	378	–	148	329	477	477	451
43/8-1	•	349	–	111	312	423	423	295
43/8A-3	⊙	210	(532)	322	210	532	532	415
44/11-1	•	293	–	41	279	320	320	70
44/14-1	•	21	–	106	–14	92	92	16
44/21-1	•	385	–	161	332	492	492	392
44/23-3	•	395	–	141	348	490	490	426
44/24-1	⊙	91	(374)	283	91	374	374	116
44/26-1	•	555	–	–44	570	526	526	579
44/29-1A	•	–108	–	–206	–39	–245	939	–245
44/7-1	•	93	–	198	27	225	225	369
47/-15-1	•	853	–	–144	901	757	757	1030
47/13-1	□	962	–	–479	1441	962	962	1060
47/13-2	•	674	–	220	600	821	821	1340
47/14-1	•	703	–	110	666	776	776	975
47/14-2	•	681	–	192	618	809	809	918
47/15-2	⊙	594	(888)	294	594	888	888	1005
47/18-1	⊖	845	1229	383	845	1229	1229	1498
47/20-1	•	830	–	84	802	887	887	1177
47/3-2	•	1024	–	20	1018	1037	1037	913
47/9-2	□	1100	–	–329	1429	1100	1100	1087
47/9B-4	•	1232	–	229	1156	1385	1385	1210
48/11-1	•	824	–	–15	829	813	813	2775
48/11-2	◇	714	–	–216	714	498	498	1021

Table 2 (continued)

Well		$-dZ_B^{\text{Neo}}$	$-dZ_B^{\text{preCh}}$	$-dZ_{p-B}^{\text{Tr}}$	$-dZ_B^{\text{Ch}}$	$-dZ_B^{\text{Tr}}$	$-dZ_B^{\text{BSh}}$	$-dZ_B^{\text{BSs}}$
48/12-1	△	–	2032	–	–	2032	2032	1696
48/13-1	△	–	2145	–	–	2145	2145	2119
48/13-2A	△	–	2220	–	–	2220	2220	2231
48/14-1	⊙	576	1961	1385	576	1961	1961	1907
48/17-1	•	601	–	–141	648	507	507	966
48/21-2	•	889	–	95	857	952	952	1324
48/22-3	•	857	–	–117	896	779	779	1209
48/6-24	△	–	2065	–	–	2065	2065	–
48/7B-4	△	–	2053	–	–	2053	2686	2053
49/12-6	⊙	92	(353)	260	92	353	353	386
49/13-1	•	249	–	99	216	315	315	–
49/16-1	⊙	511	1146	635	511	1146	1146	1814
49/17-2	•	453	–	225	378	602	602	326
49/18-3	•	404	–	82	377	459	459	298
49/2-1	•	1001	–	78	975	1053	1053	1163
49/21-5	⊙	559	1307	747	559	1307	1307	1450
49/22-1	⊙	447	(742)	295	447	742	742	1398
49/23-1	•	371	–	246	289	535	535	479
49/24-1	⊙	135	(411)	276	135	411	411	461
50/21-1	⊙	223	(537)	314	223	537	537	720
52/5-11	•	561	–	–150	611	461	461	812
53/1-2	•	483	–	75	458	533	533	775
53/12-1	•	441	–	100	408	508	508	789
53/14-1	⊙	508	(788)	280	508	788	788	975
53/19A-1	•	546	–	147	497	643	643	806
53/2-2	•	604	–	221	530	751	751	631
53/2-3	•	612	–	193	547	740	740	878
53/3-1	•	462	–	216	390	606	606	540
53/7-1	•	526	–	66	504	570	570	811
53/8-1	•	498	–	–19	505	485	485	756
54/1-1	⊙	232	823	591	232	823	823	539
54/11-1	•	295	–	167	239	406	406	–
Cleeth.	□	951	–	–304	1255	951	–	951

value by more than 400 m (8 wells) or if no Bunter Shale value is available (1 well).

4. Reconstruction of normal velocity–depth trends

4.1. The palaeo-velocity–depth plot

Prior to Neogene erosion, the Chalk Group was at maximum burial along the margins of the North Sea Basin. The Neogene erosion reduced the thickness of the overburden relative to the Chalk and the underlying Mesozoic sediments (e.g. Japsen, 1998). We can thus construct palaeo-velocity–depth plots for a pre-Chalk formation corresponding to the situation prior

to Neogene erosion by correcting the present-day depth, z , for the erosion as estimated by the Chalk burial anomalies, dZ_B (Fig. 1). By assuming that the Chalk burial anomaly is a measure of the amount of Neogene erosion, and substituting it into Eq. (1), we get:

$$z_{\text{pre-Neo}} = z - dZ_B^{\text{Ch}} \tag{3}$$

where $z_{\text{pre-Neo}}$ is an estimate of the formation depth prior to Neogene erosion (Figs. 3b–5b). In this way we can reconstruct baselines for pre-Chalk formations more easily than in plots of present depth versus velocity (Figs. 3b–5b).

Palaeo-velocity–depth plots should be analysed in a similar way to ordinary plots of velocity versus

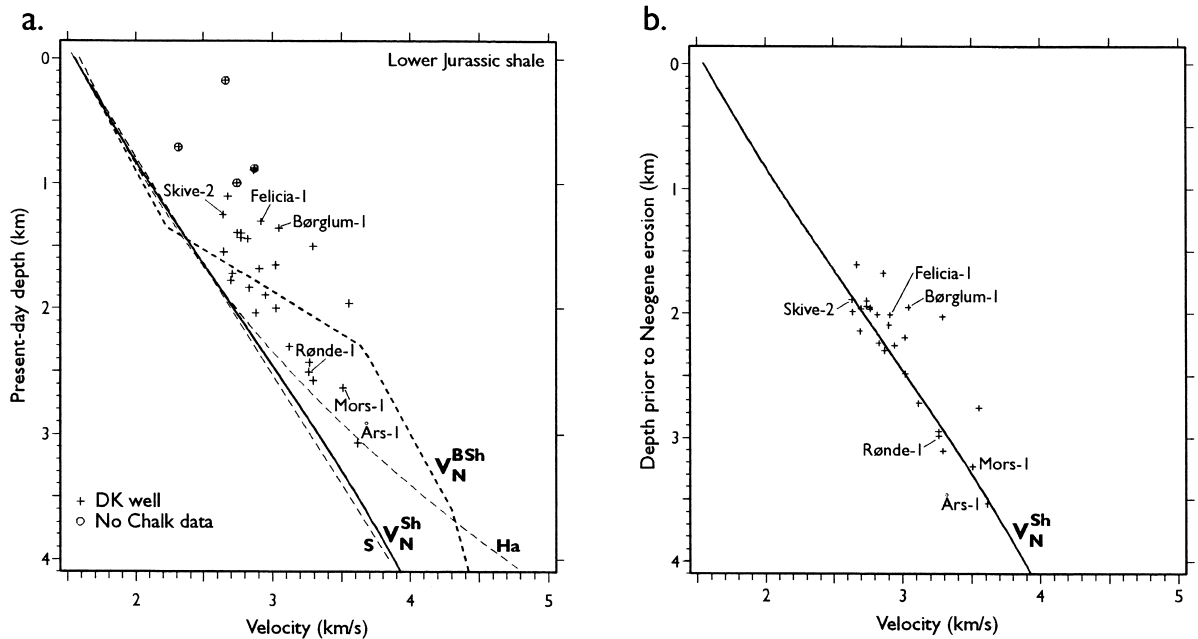


Fig. 3. Lower Jurassic shale (F-1 Member of the Fjerritslev Formation): plot of interval velocity versus midpoint depth. The shale trend, V_N^{LJur} , can be traced more easily if we correct present depths for the Neogene erosion. Note the agreement between V_N^{LJur} and the baselines of Scherbaum (1982) and Hansen (1996), and the clear distinction relative to the Bunter Shale trend. (a) Present-day depth below top of sediments. (b) Depth prior to Neogene erosion estimated by correcting the present-day depth by the Chalk burial anomaly (palaeo-velocity–depth plot). Legend: Ha, Hansen (1996) (Jurassic–Miocene shale, Norwegian Shelf); S, Scherbaum (1982) (Lower Jurassic shale, Northwest German Basin); V_N^{BSh} , Bunter Shale baseline, shown for comparison (Eq. 5); V_N , Lower Jurassic shale baseline (Eq. 4).

present-day depth for uniform lithologies as discussed by several authors (e.g. Bulat and Stoker, 1987; Hillis, 1995; Japsen, 1998). The lower velocities for a given depth in general represent data at normal compaction whereas the higher velocities reflect increasing erosion of the overburden (assuming uniform conditions and hydrostatic pressure). However, the reconstructed trend is represented by a scatter of minimum velocities for given depths, and not by the strict minimum data points due to inaccuracy in the determination of the Neogene erosion from the Chalk data. Data points of high velocities relative to the baseline in the palaeo-velocity–depth plot thus represent locations where the formation in question experienced maximum burial prior to Neogene erosion (assuming uniform conditions).

4.2. Lower Jurassic shale

The palaeo-velocity–depth plot for the Lower Jurassic shale in Fig. 3b shows a well-defined trend of data points at maximum burial (identified as the

lower bound) (for $2.6 < V < 3.6$ km/s; the Skive-2 to the Års-1 wells). A number of data points plot above the trend and presumably represent either areas where the Lower Jurassic shale was at maximum burial prior to Neogene erosion or areas where the lithology of the shale differs from mean composition (e.g. more kaolin as discussed in Section 4.3; well Børglum-1; Schmidt, 1985). The normal velocity–depth trend for the Lower Jurassic shale, V_N^{LJur} , can be approximated by a constrained, exponential transit time–depth trend of the form $1/V = ae^{-b/z} + c$ (Eq. A-1 in Appendix A)¹:

$$V_N^{LJur} = 10^6 / (460e^{-z/2175} + 185). \quad (4)$$

¹ The shale trend was found to be $10^6 / (465e^{-z/2435} + 180)$ before the revision of the Chalk baseline of Japsen (1998) (see Appendix B). The revised Chalk baseline is shifted towards shallower depths by up to 210 m relative to the original baseline. The shale trend given by Eq. (4) is thus also shifted towards more shallow depths relative to the original version, e.g. by 200 m for $z = 2$ km (compare Japsen, 1999).

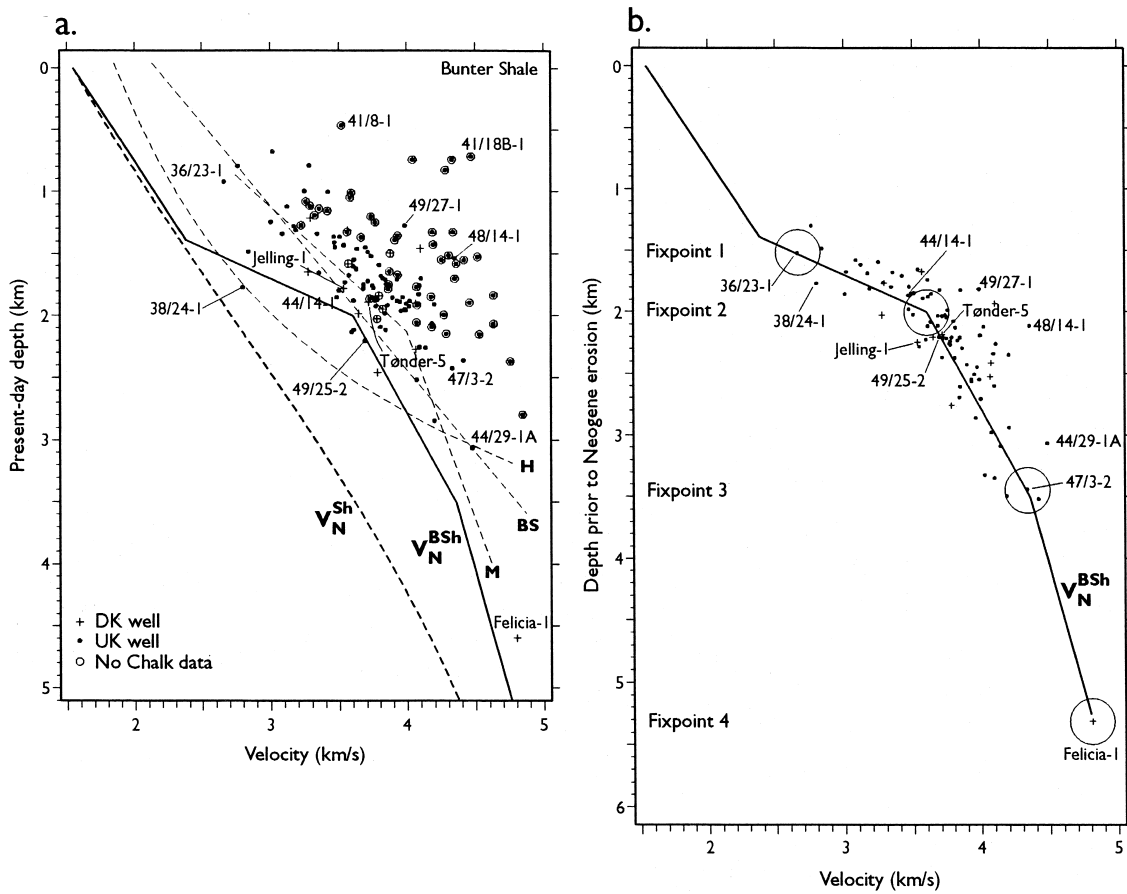


Fig. 4. Bunter Shale: plot of velocity versus midpoint depth. The Bunter Shale trend, V_N^{BSh} , can be traced more easily if we correct present depths for the Neogene erosion. The difficulty in identifying data representing normal compaction and the assignment of functional expressions that predict infinite velocity at depth has led to the suggestion of baselines that deviate substantially from that suggested here. (a) Present-day depth below top of sediments. (b) Depth prior to Neogene erosion estimated by correcting the present-day depth by the Chalk burial anomaly (palaeo-velocity–depth plot). Legend: BS, Bulat and Stoker (1987) (southwestern North Sea Basin, also H and M); H, Hillis (1995); M, Marie (1975) (approximation); V_N^{BSh} , Bunter Shale baseline (Eq. 5); V_N^{Sh} , Lower Jurassic shale baseline, shown for comparison (Eq. 4).

The trend is constrained because it fulfils reasonable boundary conditions at the surface and at infinite depth, $V_0 = 1550$ m/s and $V_\infty = 5405$ m/s. The trend has a maximum velocity–depth gradient of 0.6 m/s/m [s^{-1}] at $z = 2.0$ km.

4.3. Bunter Shale

The palaeo-velocity–depth plot for the Bunter Shale in Fig. 4b shows a trend of scattered data points at maximum burial (for $2.6 < V < 4.8$ km/s; wells 36/23-1 to Felicia-1). By contrast, the plot of

velocity versus present depth in Fig. 4a reveals no clear lower bound of data points at maximum burial. A number of data points plot clearly above the palaeo-velocity–depth trend, and thus represent areas where the Bunter Shale was at maximum burial prior to Neogene erosion or possibly areas of anomalous lithology (e.g. well 48/14-1).

The depth shift between the observed trends for the Bunter and the Lower Jurassic shale trends exceeds 1 km for $V > 3$ km/s. This shift must be related to physical differences between the two lithologies that has the word ‘shale’ in common (the

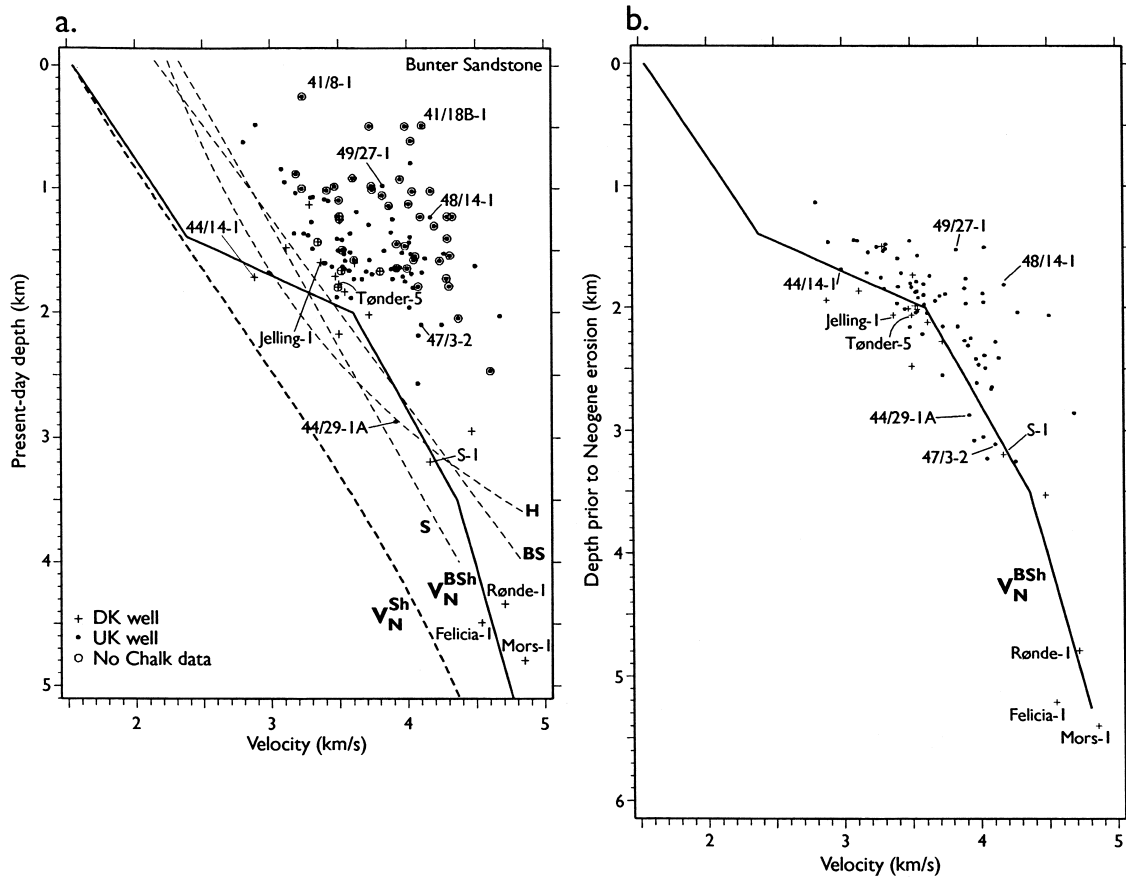


Fig. 5. Bunter Sandstone: plot of velocity versus midpoint depth. The Bunter Shale trend, V_N^{BSH} , follows the trend of Bunter Sandstone data in the plot of depths corrected for the Neogene erosion. (a) Present-day depth below top of sediments. (b) Depth prior to Neogene erosion estimated by correcting the present-day depth by the Chalk burial anomaly (palaeo-velocity–depth plot). Legend: BS, Bulat and Stoker (1987) (southwestern North Sea Basin, also H); H, Hillis (1995); S, Scherbaum (1982) (Northwest German Basin); V_N^{Sh} , Bunter Shale baseline (Eq. 5); V_N^{BSH} , Lower Jurassic shale baseline, shown for comparison (Eq. 4).

reasons for these differences are discussed in Section 5). An explanation related to a previous greater burial for all the data points defining the Bunter trend than for the Jurassic trend would imply a missing section of several kilometers of Triassic–Lower Cretaceous sediments. This implication would not be compatible with the geology of the area as discussed in Section 6.

The trend of data points at maximum burial reveals a slight curvature that reflects the decrease of the velocity gradient with depth, and this trend is approximated by three linear segments plus a fourth segment that connects the observed trend with a physically reasonable velocity at the surface (Fig.

4b). This formulation is chosen because a simpler mathematical function fails to account for the observed depth variations, and because the linear expressions for the segments are easy to compare (Eq. A-2 in Appendix A). Fixed points (or reference points) are identified along the trend to define the segments over finite intervals. Round figures are preferred to emphasise the simplicity of the model.

The first fixed point for the baseline is taken at well 36/23-1 which defines the upper left part of most shallow and rather scattered trend of data points. This fixed point plots just above well 38/24-1 where the Chalk burial anomaly is +223 m and thus indicates a minor undercompaction of the sediments.

The second fixed point is taken to be 3600 m/s at 2000 m, just above a cluster of data points below which depth a slower increase of velocity with depth is observed (e.g. well 49/25-2, which has a zero Chalk burial anomaly, and well Tønder-5). The third fixed point is taken to be 4350 m/s at 3500 m at the deepest part of the trend (e.g. well 47/3-2). The deepest data point, from the Felicia-1 well, is taken as the fourth fixed point.

If we let the upper part of the normal trend coincide with the trend of the Lower Jurassic shale to arrive at a velocity at the surface close to that of water, 1550 m/s, we get the following normal velocity–depth trend for the Bunter Shale, V_N^{BSh} :

$$\begin{aligned} V_N^{\text{BSh}} &= 1550 + 0.6z, & 0 < z < 1393 \text{ m} \\ V_N^{\text{BSh}} &= -400 + 2z, & 1393 < z < 2000 \text{ m} \\ V_N^{\text{BSh}} &= 2600 + 0.5z, & 2000 < z < 3500 \text{ m} \\ V_N^{\text{BSh}} &= 3475 + 0.25z, & 3500 < z < 5300 \text{ m} \end{aligned} \quad (5)$$

This trend indicates a pronounced variation of the velocity gradient with depth: the gradient is as high as 2 m/s/m for depths around 2 km, from where it decreases gradually with depth to 0.5 and then 0.25 m/s/m. The gradient is taken to be 0.6 m/s/m in the upper part to arrive at a physically reasonable velocity at the surface.

4.4. Bunter Sandstone

The palaeo-velocity–depth plot for the Bunter Sandstone in Fig. 5b has a trend of data at maximum burial that coincides approximately with the normal trend for the Bunter Shale ($3.0 < V < 4.3$ km/s; wells 44/14-1 to S-1). Several wells plot along the Bunter trend for both the Bunter Shale and Sandstone (e.g. wells 44/14-1, 47/3-2, and Tønder-5) or plot equally much above the trend (e.g. wells 48/14-1 and 49/27-1). Data from shale is, however, preferable to those from sandstone for studies of maximum burial for several reasons: shale porosity is less affected by diagenetic processes, shale does not act as an aquifer with the consequent porosity variations, and shale may be more uniformed in regards to both grain size and to mineralogy. The wide range of velocities for the Bunter Sandstone, for moderate depths (e.g. 2 km) may thus be caused by differences in primary lithology or diagenesis (Fig. 5b). Rather

than proposing a specific baseline for the Bunter Sandstone, the trend formulated for the Bunter Shale is suggested to be a reasonable approximation for the present data set ($V > 2.8$ km/s). In this way Bunter Sandstone burial anomalies can be used to place an upper limit on estimates of erosion based on Bunter Shale data.

4.5. Comparison with baselines suggested by other authors

The increase of velocity with depth must approach zero at depth for any lithology. However, the models discussed below — apart from that of Marie (1975) — imply a constant velocity gradient with depth (Scherbaum, 1982; Bulat and Stoker, 1987) or an increasing value (Hillis, 1995; Hansen, 1996) (see the discussion in Appendix A). Consequently, there is an increasing difference with depth between these models and those presented here, a fact that underlines the importance of the mathematical formulation of the baseline (Figs. 3a–5a). Furthermore, the baselines suggested by the various authors are all defined from a selection of the data points for which the lowest velocity at a given depth is assumed to represent normal compaction. The recognition of the absolute baseline level thus becomes very sensitive to the presence — or absence — within a data set of data points representing normal compaction, and consequently to the evaluation of outliers.

A linear velocity–depth trend for Lower Jurassic shale in the Northwest German Basin was established by Scherbaum (1982). This trend is within 100 m from that established here for the adjacent Danish Basin for $z < 4$ km (Eq. 4; Fig. 3a). This agreement may be taken as evidence for the level of erosion estimated from Chalk velocities (see Appendix B). Jankowsky (1962) presented a similar trend for Lower–Middle Jurassic shales in the same area. It is also noteworthy that the shale trend given by Eq. (4) is less than 100 m apart (for $z < 2.4$ km) from the simple, exponential transit time–depth model for Jurassic–Miocene shale on the Norwegian shelf suggested by Hansen (1996). The model of Hansen predicts infinite velocity at great depth, and the deviation thus exceeds 250 m for $z > 2.9$ km.

The Bunter Shale trend of Marie (1975) is about 500 m more shallow than the trend suggested here

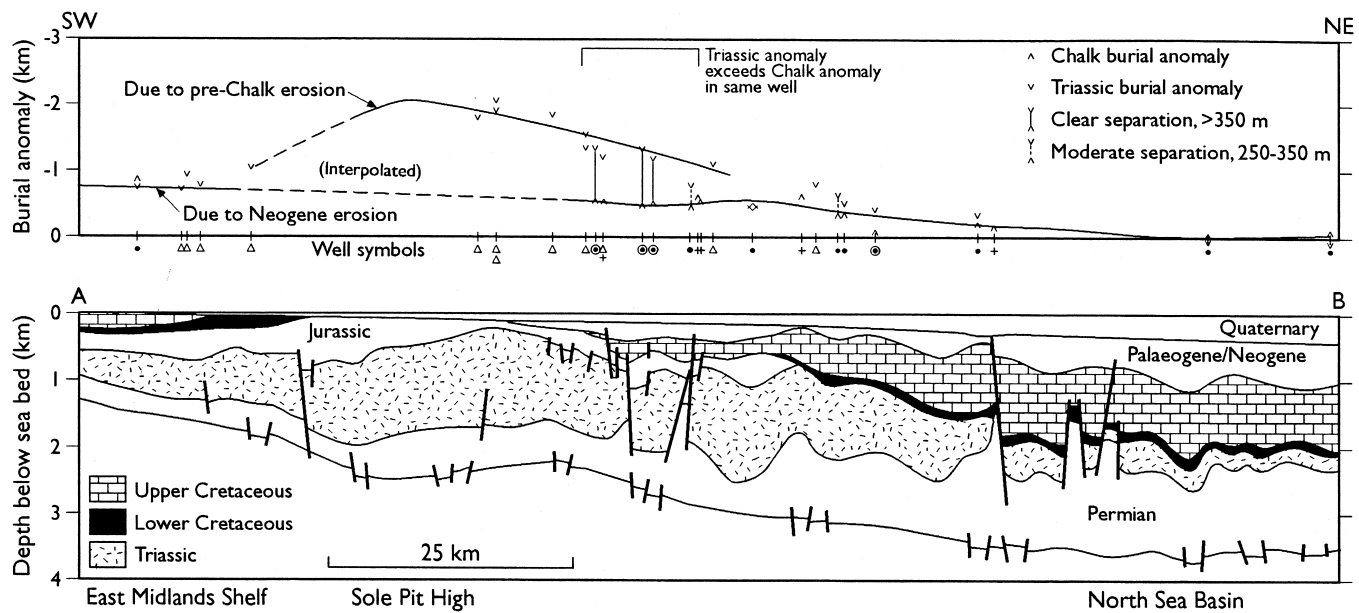


Fig. 6. Profile across the Sole Pit axis (location indicated on Figs. 8 and 9). (Upper panel) Burial anomalies for the Chalk and the Triassic estimated in wells within 20 km from the profile, and the interpreted levels of erosion due to Neogene and pre-Chalk erosion from the maps in Figs. 8 and 9. The separation of the erosional events is based on the clear difference close to the Sole Pit axis between the burial anomalies for two levels estimated in the same wells, and on the much higher level of the anomalies along the axis where the Chalk is absent. Well symbols referring to the estimated burial anomalies are defined in Table 2; compare Fig. 7. (Lower panel) Depth profile illustrating how successively older Mesozoic sediments subcrop the Quaternary towards the Sole Pit axis (Cameron et al., 1992). Note the absence of Lower Cretaceous sediments between the Chalk and the Jurassic to the east of the Sole Pit axis where the well velocity data indicate deep pre-Chalk erosion.

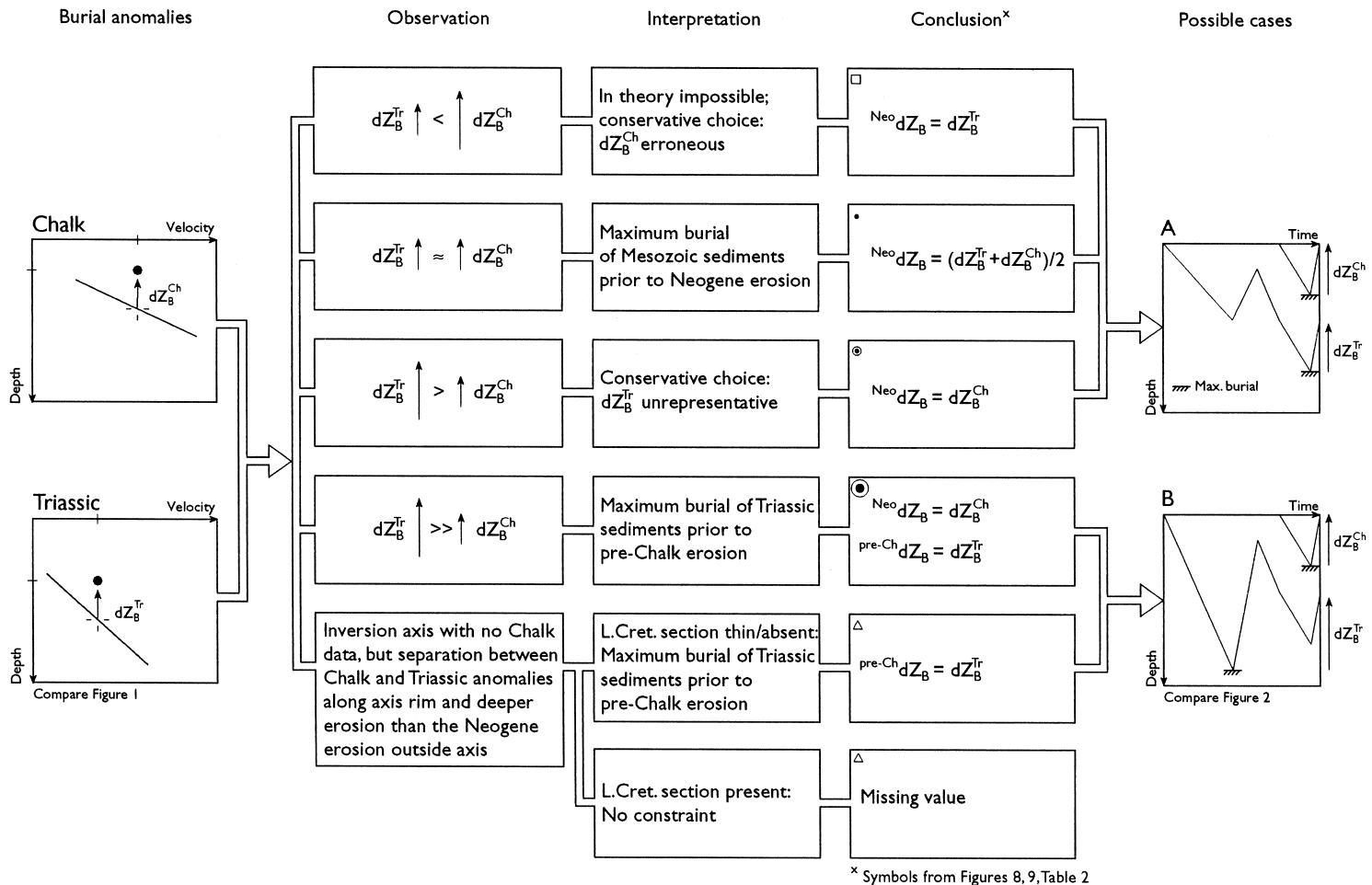


Fig. 7. Decision tree for the investigation of the burial history of the Mesozoic succession based on burial anomalies for the Chalk and a Triassic formation in the same well, dZ_B^{Ch} and dZ_B^{Tr} . Where the Triassic formation experienced its maximum burial prior to the deposition of the Chalk it is possible to separate the magnitudes of the Neogene and the pre-Chalk erosion, $^{Neo}dZ_B$ and $^{pre-Ch}dZ_B$, respectively (case B). Where the entire Mesozoic succession was at maximum burial prior to Neogene erosion the burial anomalies for the two levels become identical (case A).

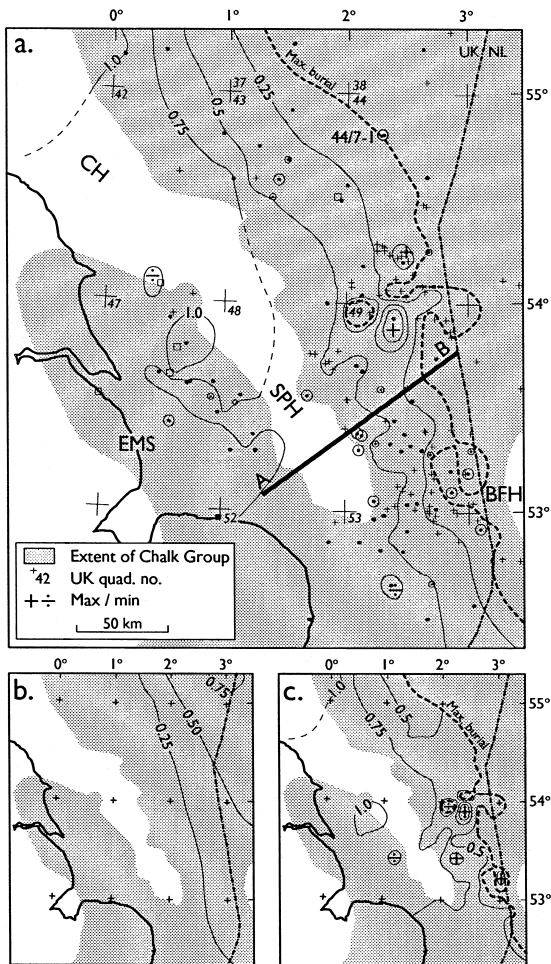


Fig. 8. Estimate of missing section removed by Neogene erosion in the southwestern North Sea Basin. Contour interval 0.25 km. A thick missing section is mapped towards E and NE where Quaternary reburial reduces the magnitude of the burial anomaly. (a) Magnitude of the burial anomaly due to Neogene erosion; cut-off for maximum burial is taken for burial anomalies >100 m (Table 2). (b) Post-exhumational burial approximated by the thickness of the Quaternary (Cameron et al., 1992; Japsen, 1998). (c) Missing section (Eq. 2). Legend: BFH, Broad Fourteens High; CH, Cleveland High; EMS, East Midlands Shelf; SPH, Sole Pit High. Detail of Fig. 3. Well annotation in Fig. 7 and Table 2. Profile AB in Fig. 6.

for $z < 5$ km (Fig. 4a; Eq. 5). This is because the reference level of Marie (1975) was based on data points outside structural highs in the UK southern North Sea, and the Neogene exhumation of these areas was not taken into account. Linear velocity–depth trends were estimated by Bulat and Stoker

(1987) for the Bunter Shale and Sandstone in the UK southern North Sea. Both these trends are shifted towards high velocities ‘to avoid generating excessively high values of apparent uplift’ (Bulat and Stoker, 1987, p. 296). A linear transit time–depth trend for the Bunter Shale in the UK southern North Sea was established by Hillis (1995). This trend is within 500 m of the trend suggested here for $1.9 < V < 4.3$ km/s, whereas it deviates more for higher velocities. Hillis (1995) defined his trend by data from wells 38/24-1 and 44/29-1A. In the present study, the Mesozoic succession in both these wells is found to be close to normal compaction. However, whereas the burial anomalies for well 44/29-1A for the Bunter Sandstone and the Chalk are close to zero, the data point for the Bunter Shale plots more about 1 km above the Bunter trend. Consequently, the Bunter Shale data for well 44/29-1A is considered unrepresentative or possibly erroneous.

Earlier suggestions for the baseline of the Bunter Sandstone are close to the trend suggested here for velocities around 3.5 km/s (Fig. 5a) (Scherbaum, 1982; Bulat and Stoker, 1987; Hillis, 1995). Hillis (1995) defined his baseline for the Bunter Sandstone by data from wells 44/29-1A (see above) and 44/14-1 for which the Mesozoic succession is found to be close to maximum burial in the present study (Fig. 5a). However, beyond these reference points, the mathematical formulation chosen by Hillis (1995) leads to an increasing deviation between his trend and the one suggested here.

5. Differences in clay mineralogy

The steep increase in velocity for the Bunter Shale around a depth of 2 km differs from the slow increase for Lower Jurassic shale, for Upper Jurassic–Miocene shale in the North Sea, and for shales in other basins (Figs. 3b and 4b) (e.g. Hottmann and Johnson, 1965; Hansen, 1996). The corresponding shift in depth between the Lower Jurassic and the Bunter shale trends exceeds 1 km for $V > 3$ km/s. The higher velocity of the Bunter Shale at depth indicates that compaction leads to better grain contacts in the Bunter Shale than in the Lower Jurassic shale.

The Bunter Shale in the southern North Sea is stratigraphically equivalent to the mudstones of the

Smith Bank Formation in the central North Sea, and both accumulated on a continental plain during a hot, semi-arid climate (Cameron, 1993; Johnson et al., 1994). Whereas little is known about the clay mineralogy of the Triassic sediments in the southern North Sea, the Smith Bank Formation is characterised by its kaolin content (Jeans, 1995). The equivalent Bunter Shale is thus likely to be characterised by a high kaolin content, because this mineral typically is associated with continental sediments, and indicative of proximity of the source area (Lindgreen, 1991; Jeans, 1995). The Lower Jurassic Fjerritslev Formation, however, was deposited in a marine environment (Michelsen, 1989), and its clay mineralogy is dominated by smectite/illite in distal parts of the basin (H. Lindgreen, personal communication), whereas kaolin is prominently close to the Fennoscandian Shield (e.g. Pedersen, 1985; Schmidt, 1985).

Kaolin that has little adsorbed water builds up thick flakes that are up to a thousand times larger than the smectite/illite particles that are separated by water molecules (Bailey, 1980; H. Lindgreen, personal communication). The interlayer water is adsorbed to the smectite/illite particles even during deep burial (van Olphen, 1966), and is likely to lead to weak mechanical grain contacts, and thus to the low sonic velocity of the Lower Jurassic shale. Mechanical adjustment of the kaolin flakes during compaction would lead to increased contact between the flakes, and thus to the observed rapid increase in velocity observed in the Bunter Shale at around a burial depth of 2 km. A shale, dominated by well-packed, silicate flakes of kaolin, could thus achieve rock physical properties similar to those of a consolidated sandstone.

6. Possible detection of pre-Cenozoic erosion along the Sole Pit axis

6.1. Comparison of burial anomalies for Mesozoic formations

The lowermost and the uppermost parts of the Mesozoic succession may or may not have been simultaneously at maximum burial in the south-western North Sea where different erosional events oc-

curred during the Mesozoic and the Cenozoic (Fig. 1). The Chalk was at maximum burial prior to Neogene erosion. Maximum burial of the Triassic sediments may also have occurred then or may have occurred prior to a pre-Chalk erosional event. We can thus investigate the burial history of a pre-Chalk formation by comparing its burial anomalies with these for the Chalk in the same wells. Comparison of the burial anomalies may lead to two results, either:

(A) The burial anomalies for the two units are identical. In this case both units have experienced maximum burial prior to Neogene erosion, and subsequently an identical reduction of overburden thickness (Fig. 1A); or

(B) The magnitude of the burial anomaly for the deeper level is greater than for the upper unit. In this case the pre-Chalk formation experienced maximum burial prior to the deposition of the Chalk because the magnitude of the pre-Chalk burial anomaly exceeds the Cenozoic erosion known from Chalk data (Fig. 1B). Consequently, the maximum burial of the pre-Chalk formation and the subsequent erosion of its overburden must have taken place prior to the deposition of the Chalk.

The magnitude of the burial anomaly for the Triassic sediments only exceeds the burial anomaly for the Chalk clearly in a number of wells along the east flank of the Sole Pit axis (the above case B) (Fig. 6). Furthermore, a very high level of the Triassic anomalies (2 km) occurs continuously along the axis where the Chalk is absent, but returns to values similar to those of the Chalk further west. These observations may be explained if the maximum burial of the Triassic succession along the inversion zone occurred during the Mesozoic.

A separation of the magnitudes of the Neogene and the pre-Chalk erosion, ${}^{\text{Neo}}dZ_B$ and ${}^{\text{pre-Ch}}dZ_B$, from the two sets of burial anomalies may thus be pursued (the decision tree is illustrated graphically in Fig. 7; Table 2). Contiguous areas of anomalous burial anomalies are mapped along the Cleveland and the Sole Pit Highs and west of the Broad Fourteens Basin (Figs. 8a and 9a). The former of these areas is only mapped where Lower Cretaceous sediments are absent (see below for a discussion of the timing of the possible erosional phase).

The above analysis may also be carried out in terms of the palaeo-burial-anomaly, dZ_{p-B}^{Tr} , for the

Triassic formation. This quantity is introduced here as the difference between burial anomalies for the Triassic formation and for the Chalk (see Tables 1 and 2). The palaeo-burial-anomaly thus corresponds to the burial anomaly of the Triassic formation prior to Neogene erosion.

6.2. *Timing of deep Mesozoic erosion*

More than 2 km of sediments were eroded prior to the deposition of the Chalk along the Sole Pit axis according to the above interpretation of the sonic data. Evidence for and timing of such deep erosion should be available from the stratigraphic record. In an early analysis, Glennie and Boegner (1981) concluded that uplift of the Sole Pit Basin occurred during the Early and in the latest Cretaceous on the northeastern and the southwestern sides of the basin, respectively. However, van Hoorn (1987) found that the large amount of missing overburden (> 1.5 km) along the Sole Pit axis that had been estimated in previous studies could not be accommodated within the Triassic–Jurassic sequence. van Hoorn (1987) suggested instead that great thicknesses of now partly missing Lower Cretaceous sediments may have been deposited at least locally in the area, and that the first phase of erosion occurred during the Turonian. The inversion movement led to the observed thinning and onlap of the Turonian–Lower Campanian Chalk onto the Sole Pit High where crestal wells encountered Late Campanian to Maastrichtian Chalk on top of the Jurassic sequence (van Hoorn, 1987) (compare Fig. 75 in Cameron et al., 1992). Chalk may thus never have been deposited over parts of the Sole Pit High.

Maximum burial of the Triassic sediments may thus have occurred prior to either an Early or a Late Cretaceous erosional event as evidenced by hiatus covering both Early Jurassic–Late Cretaceous and Triassic–Jurassic intervals at different locations in the southwestern North Sea (compare Cameron et al., 1992). Along the Sole Pit axis, 950 m of Jurassic, and 900 m of Lower Cretaceous sediments have been proven (Cameron et al., 1992). These numbers make Late Cretaceous erosion in the order of 2 km plausible, especially taking into account that the major movements of subsidence and uplift are to be expected along the main fault bounding the Sole Pit axis (compare van Hoorn, 1987). In the present

analysis, deep erosion along the Sole Pit axis is mapped only where the Lower Cretaceous is absent, and sediments of Early Jurassic–Late Cretaceous age may have been removed during Late Cretaceous erosion (Cameron et al., 1992). West of the Broad Fourteens High, Lower Cretaceous sediments overlie the Triassic succession, and erosion may have occurred in the Early Cretaceous.

6.3. *Magnitude of Cenozoic erosion*

The burial anomaly due to Neogene erosion is mapped in Fig. 8a (compare Fig. 7; Table 2). The map shows an increase from zero burial anomaly in quadrants 37 and 44 and along the limitation of the Dutch sector to a maximum anomaly of about 1.1 km on the East Midlands Shelf, and the contours generally parallel the English coast (Fig. 8). Local variation of the anomaly may be due to lithological variations and data errors, but also to uplift by salt diapirism and to reburial in rim-synclines (e.g. van Hoorn, 1987).

The resulting map of the missing section due to Neogene erosion (Fig. 8c) equals the map of the overburden reduction corrected for the Quaternary reburial as estimated from a contour map (Fig. 8b; Eq. 2). Thick missing sections are thus mapped towards the north-east and east because the Quaternary thickness increases towards the basin centre and exceeds 500 m where the Chalk is normally compacted. At the basin margin where the Quaternary cover is thin, the removed sediments are likely to have been of mainly Palaeogene age (Japsen, 1997, 1998). Further into the basin, along the line of maximum burial of the Chalk, a succession of less than 0.5 km is predicted to have been removed. This result is consistent with the basal Pliocene unconformity in the western North Sea (Cameron et al., 1992), evidenced by the absence of Miocene deposits in well 44/7-1 (c.f. Japsen, 1997).

Towards the basin centre, the thickness of the removed section is gradually reduced, and must be zero below the Quaternary depocentre where sedimentation was continuous throughout the late Cenozoic (Gatliff et al., 1994). The calculation of the missing section becomes very sensitive to minor errors in the estimates in the burial anomaly and in the Quaternary reburial where the Mesozoic succession is close to maximum burial.

6.4. Magnitude of Mesozoic erosion

Triassic sediments along the Sole Pit axis appear to have been at maximum burial prior to an erosional phase pre-dating the deposition of the Chalk (Fig. 9a;

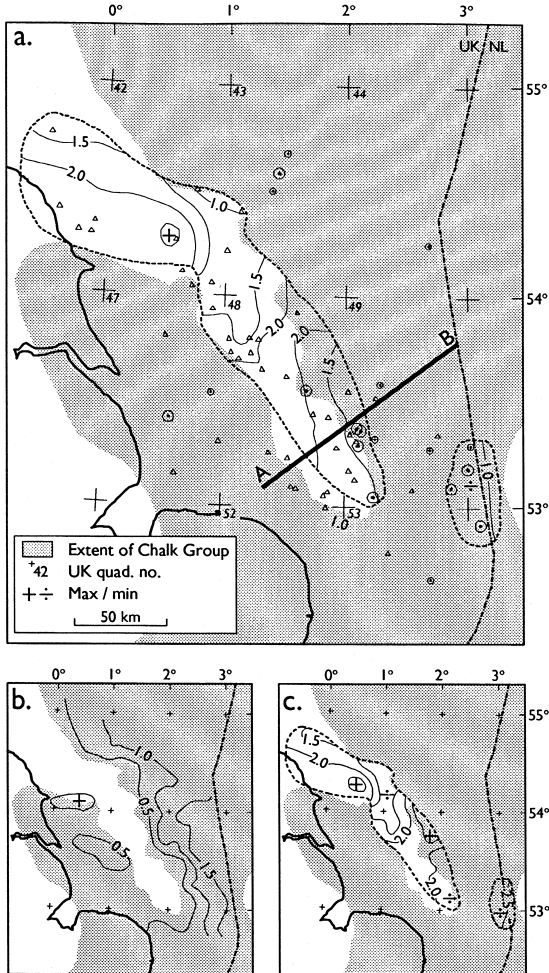


Fig. 9. Estimate of missing section removed during pre-Chalk erosion in the southwestern North Sea Basin. Contour interval 0.5 km. More than 2 km of Mesozoic sediments have been eroded along the Sole Pit axis and west of the Broad Fourteens Basin. (a) Magnitude of the burial anomaly due to pre-Chalk erosion (Table 2). (b) Post-exhumational burial approximated by the thickness of the post-Jurassic sediments (Day et al., 1981). (c) Missing section (Eq. 2). The dashed line indicates the area where the magnitude of the Triassic burial anomaly exceeds the level of the Chalk burial anomaly and where the Lower Cretaceous section is thin or absent. Detail of Fig. 3. Well annotation in Fig. 7 and Table 2. Profile AB in Fig. 6.

Table 2). The erosion exceeds 2 km over the Cleveland and Sole Pit highs within an area where Lower Cretaceous sediments are absent. The magnitude of the Triassic burial anomaly almost reaches 1 km west of the Broad Fourteens High.

To estimate the section removed by pre-Chalk erosion, the post-exhumational reburial is approximated by the thickness of the post-Jurassic deposits (Fig. 9b; Eq. 2). Along the Cleveland and Sole Pit Highs, the Lower Cretaceous is absent within the mapped area, and the correction for reburial thus comprises only the Chalk and the Quaternary deposits. The resulting map of the missing section shows less relief than the burial anomaly map because the thickness of the post-Jurassic succession increases away from the inversion axis (up to 1.5 km; Fig. 9c). The missing section is estimated to exceed 2 km along the Cleveland and Sole Pit highs, and west of the Broad Fourteens Basin.

6.5. Comparison with other studies

Marie (1975) estimated a maximum difference of 1800 m between present and maximum burial for the Bunter Shale from velocity data for the Cleveland and Sole Pit highs. The two maxima mapped by Marie correspond to the pattern established in this study, only the magnitude is about 500 m smaller than estimated here. This difference reflects the level of the Neogene erosion of the area. This late phase of erosion was not taken into account by Marie who based the reference level on data points outside the structural highs. Similar estimates of erosion based on vitrinite reflectance data were presented by Cope (1986).

Bulat and Stoker (1987) documented regional Neogene erosion of the UK southern North Sea. These authors estimated the magnitude of the erosion by the median burial anomaly for several stratigraphic units, even though they found that data from stratigraphically older units gave higher anomalies. Bulat and Stoker's (1987) analysis was influenced by expectations about the magnitude of the erosional episodes in the area and by the application of baselines that predicted too high velocities, and consequently underestimated the reduction in overburden thickness.

Hillis (1995) found that Cenozoic erosion masked the effect on velocity–depth data of any Mesozoic erosional event in the UK southern North Sea. Hillis (1995) underestimated burial anomalies for the Triassic succession because his baseline predicts too high velocities at depth (Figs. 4 and 5) (see the discussion on velocity–depth trends in Appendix A).

6.6. Other factors than burial depth affecting velocity anomalies

Strike–slip movements along the Dowsing Fault Zone bounding the Sole Pit Basin towards south-west have been suggested by several workers (compare van Hoorn, 1987). However, the inferred burial anomalies for the Bunter Shale of up to 2 km correspond to velocity anomalies about 1 km/s relative to normal velocities of 3.5 km/s, and to porosity anomalies about 15% based on Wyllie's equation. Furthermore, the burial anomalies based on sonic data are in accordance with estimates of removed overburden based on vitrinite reflectance data that primarily reflect heat flow variations (Cope, 1986). Regional tectonic stress is thus only likely to explain a minor part of the observed overcompaction.

Heat flow anomalies along the inversion zone could be a contributing factor to the burial anomalies in the order of 1.5–2 km observed from sonic and vitrinite data. Heat flow variations may, however, typically contribute only about 200 m to estimates of eroded overburden based on vitrinite data (Torben Bidstrup, personal communication). Moreover, whereas the influence of heat flow on vitrinite reflectance is primary, the influence on sonic velocities is only secondary. The observed agreement between burial anomalies based on both data sets thus suggests that the anomalies reflect a factor of primary influence on both parameters; i.e. depth of burial.

7. Discussion and conclusions

The identification of the normal velocity–depth trend for Chalk makes possible the reconstruction of baselines for relatively homogenous pre-Chalk formations in the North Sea Basin. This may be done through the construction of palaeo-velocity–depth plots that correspond to the situation prior to Neo-

gene erosion, when the formation was at maximum burial at more locations. In these plots, present-day depths of burial are corrected for Neogene erosion as estimated from Chalk velocities (see the revision of the Chalk baseline suggested by Japsen, 1998 in Appendix B). The reconstructed trends can then be applied to estimate erosion in areas where the Chalk is absent or to compare estimates of erosion for different stratigraphic levels in the same well. Previous workers have cross-plotted burial anomalies for different units to check validity of the estimated erosion (Bulat and Stoker, 1987; Hillis, 1995). These authors have thus implicitly assumed simultaneous maximum burial of the units, and have not utilised the results in a geologic model as the palaeo-velocity–depth plot.

Baselines for Lower Jurassic shale and for the Bunter Shale are reconstructed here by applying this procedure. The baseline for the Bunter Sandstone is approximated by the Bunter Shale trend for the relevant velocity interval. An immediate check on the reliability of the results may be found in the facts that the two resulting baselines reveal two distinct levels, and that both converge towards upper velocity limits with increasing depth. Furthermore, the agreement between different baselines suggested for shales dominated by smectite/illite should be noted (see Japsen, 1999). Most of the previously suggested baselines for these formations predict higher velocities over considerable depth intervals compared to the solutions presented here, and this has led to underestimation of eroded overburden, frequently by more than 500 m. The reason why the baseline for Lower Jurassic shale has been more successfully defined in previous studies than that of the Bunter Shale is most likely that the shape of the Jurassic trend is less complex and thus more easily approximated by simple mathematical expressions. Influence of clay mineralogy on the velocity–depth relation for shale formations is suggested here for the first time. Consequently, shale compaction studies should be carried out relative to trends for the dominant clay mineralogy.

This study indicates differences in the timing of maximum burial of different levels within the Mesozoic succession based on constrained velocity–depth trends for these formations. The estimated overburden reduction for the Triassic level exceeds that of

the Chalk along the Cleveland and Sole Pit highs and west of the Broad Fourteens High. There, the Triassic sediments are suggested to have been at maximum burial prior to erosion of more than 2 km of sediments, probably during the Late Cretaceous and the latest Jurassic, respectively. The influence of lateral variations in stress and heat flow on the estimated burial anomalies is found to be minor compared to those of overburden reduction. Outside the inversion axis, the overburden has been equally eroded relative to the Chalk and the Triassic successions, and this leads to the conclusion that the entire Mesozoic succession was at maximum burial prior to regional, Neogene erosion. Neogene erosion has removed less than 0.5 km of mainly Neogene sediments along the upper Cenozoic depocentre of the North Sea Basin, increasing to c. 1 km of mainly Palaeogene deposits on the East Midlands Shelf. Estimation of the missing section could be improved by incorporating detailed information about the thickness of the Quaternary deposits and by performing basin modeling on vitrinite reflectance data.

Acknowledgements

The study was financed by the Carlsberg Foundation and GEUS. Petroleum Information (Erico) is thanked for placing Chalk velocity data from UK wells at my disposal. I want to thank my colleagues Torben Bidstrup for his competent comments, Holger Lindgreen for his instructions and suggestions about clay mineralogy, as well as Jim Chalmers and Kai Sørensen for many useful comments. Important points made by referees helped me focus the manuscript.

Appendix A. Mathematical formulations of velocity–depth trends

Several mathematical formulations have been applied to represent the increase of velocity with depth, all of which express linearity between different transformations of velocity and depth. The formulations relevant for this paper are discussed below.

A linear velocity–depth function has been used by several workers for different lithologies (e.g.

Scherbaum, 1982; Bulat and Stoker, 1987; Japsen, 1993):

$$V = V_0 + kz$$

where V_0 is the velocity at the surface, and k [m/s/m] is the velocity–depth gradient.

Hillis (1995) applied a linear function between transit time, $tt = 1/V$ [s/m = 0.3048 s/ft] and depth for chalk, sandstone and shale:

$$tt = tt_0 + qz,$$

where tt_0 is the transit time at the surface, and q [s/m²] is the negative transit time–depth gradient (c.f. Al-Chalabi, 1997).

Baselines for shale have often been approximated by a simple exponential model for the reduction of transit time with depth (e.g., Hottmann and Johnson, 1965; Hansen, 1996):

$$tt = tt_0 e^{-z/b_1},$$

where b_1 [m] is an exponential decay constant.

The above three formulations are all first order approximations in either the $V - z$, $tt - z$ or $\ln(tt) - z$ plane. They all predict velocity to approach infinity for $z \rightarrow \infty$. The first formulation predicts the gradient to be constant, and the other two imply the gradient to increase with depth. While this may be valid for a depth interval, the increase in velocity with depth must inevitably reach a maximum at some depth.

A constrained, exponential transit-time–depth model was suggested for shale by Chapman (1983), and applied for sand/shale series by Heasler and Kharitonova (1996):

$$tt = (tt_0 - tt_\infty) e^{-z/b_2} + tt_\infty \quad (\text{A-1})$$

where tt_∞ is the transit time at infinite depth, and b_2 [m] is an exponential decay constant (c.f. Al-Chalabi, 1997). This formulation is linear in the $\ln(tt - tt_\infty) - z$ plane, and implies that $tt \rightarrow tt_\infty$ and the velocity–depth gradient, $k \rightarrow 0$ for $z \rightarrow \infty$. The equation is thus a convenient, though not a universal baseline formulation.

Finally, a segmented linear velocity–depth function was suggested for the North Sea Chalk by Japsen (1998). The continuous function is defined over a depth interval divided into n segments:

$$V = V_{0i} + k_i z, \quad z_{ai} < z < z_{bi}, \quad (\text{A-2})$$

where V_{0i} is the velocity predicted at the surface and k_i is the velocity–depth gradient of the i th segment defined for depths between z_{ai} and z_{bi} .

Appendix B. A revised normal velocity–depth trend for the North Sea Chalk

Japsen (1998) published a normal velocity–depth trend for the Chalk Group based on an analysis of 845 wells throughout the North Sea Basin and ODP data. For the shallowest part of the trend, no data representing normal compaction were found for the Chalk of the North Sea Basin, so sonic log data from Eocene to Recent ooze and chalk deposits from a stable platform were used to guide the trend (Urmos et al., 1993). At intermediate depths, Japsen (1998) applied qualitative arguments to identify North Sea data representing normal compaction along the lower bound for velocity–depth data for which the effect of overcompaction due to erosion is minimum. At greater depths, data representing normal compaction were identified along the upper bound where the effect of undercompaction due to overpressuring is a minimum.

I have found additional geological constraints that refine the identification of reference data at intermediate depths where the influence of erosion and overpressuring is difficult to ascertain. Because the sonic method identifies deviations from maximum burial, post-erosional reburial of a formation will reduce its observable burial anomaly; e.g. a pre-Quaternary erosion of 500 m will be masked by a subsequent Quaternary reburial of 500 m (Eq. 2). This implies that, where the Quaternary is thick, even minor deviations from maximum burial due to Neogene erosion may correspond to a substantial missing section. Deep erosion is, however, not likely where the base-Quaternary hiatus is minor, e.g. where the Quaternary is underlain by Neogene sediments.

Normally-compacted Chalk is thus likely to be found in areas where the Quaternary is thick, Neogene deposits are present and pressure is hydrostatic. Consequently, the normal velocity–depth trend for the North Sea Chalk should follow the upper bound for data from such areas, whereas data representing undercompaction due to overpressuring should plot below the trend (Fig. 10). A revised baseline has

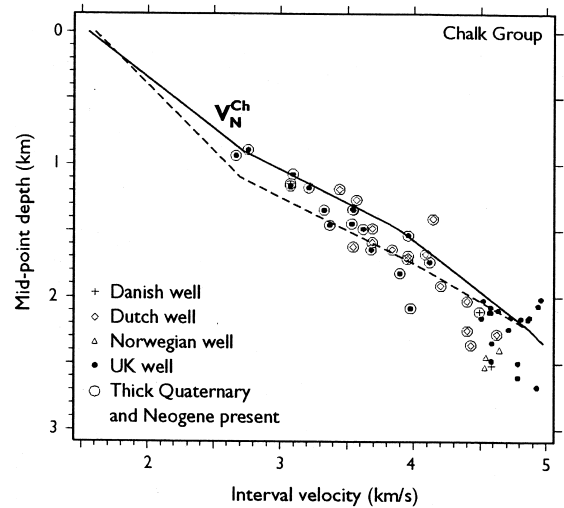


Fig. 10. Chalk group: plot of interval velocity versus mid-point depth. The revised Chalk baseline, V_N^{Ch} , follows the upper bound for wells where thick Quaternary and Neogene sediments are present (Eq. B-1). Even a small deviation from maximum burial for these wells would imply that a pronounced section should be missing because Quaternary reburial masks the true magnitude of the Neogene erosion (Eq. 2). Data have been used from wells from Dutch quadrants E, K, L, M, and P, UK quadrants 29, 37, 38, 44 and the Danish wells L-1 and S-1 and wells with maximum Chalk velocity for $z > 2000$ m (Fig. 2). The dashed line indicates the original baseline of Japsen (1998).

been defined by such maximum velocity data for $900 < z < 1700$ m. The revised trend lines up with the maximum velocity data used to define the original trend for $z > 2000$ m, and with a velocity at the surface of 1550 m/s. The following revised normal velocity–depth trend for the North Sea Chalk is thus suggested:

$$\begin{aligned} V_N^{\text{Ch}} &= 1550 + 1.3z, & z < 900 \text{ m} \\ V_N^{\text{Ch}} &= 920 + 2z, & 900 < z < 1471 \text{ m} \\ V_N^{\text{Ch}} &= 1950 + 1.3z, & 1471 < z < 2250 \text{ m} \\ V_N^{\text{Ch}} &= 2625 + z, & 2250 < z < 2875 \text{ m} \end{aligned} \quad (\text{B-1})$$

The fourth of the above segments is unchanged from the original trend, in which the upper three segments were formulated as $1600 + z$, $500 + 2z$, and $937.5 + 1.75z$ (Japsen, 1998). The trend is defined over intervals of depth, whereas the inverted function used for estimating maximum burial is defined over intervals of velocity (Eq. 1). The revised

trend is shifted towards shallower depths by a mean of 160 m for the velocity interval affected by the revision and where North Sea data are found, $2100 < V < 4875$ m/s; the maximum shift is 210 m for $2920 < V < 3920$ m/s.

The increase of velocity with depth is assessed to be 1.3 m/s/m [s^{-1}] for the upper segment rather than the original value of 1 m/s/m that was based on a sonic log at ODP Site 807. This deviation between the velocity gradients for pelagic carbonates at shallow depth may be explained by differences in the effective stress exerted by the overlying sediments due to density variations, because porosity reduction, and hence velocity increase, is governed by mechanical compaction (Borre and Fabricius, 1998; Japsen, 1998).

We can approximate the steady porosity decrease throughout the upper 1100 m of pelagic carbonate sediments by two half sections at 60% and 50% porosity at ODP Site 807 (Urmos et al., 1993; Borre and Fabricius, 1998). The average density for the section is thus approximately 1.78 g/cm^3 (assuming $\rho_{\text{calcite}} = 2.71 \text{ g/cm}^3$ and $\rho_{\text{water}} = 1.02 \text{ g/cm}^3$), compared with a typical density of 2.05 g/cm^3 for normally compacted Cenozoic siliciclastics in the upper kilometre of the sedimentary column in the North Sea (Japsen, 1998). The velocity increase with depth should thus be higher in the North Sea where the overburden is denser than in an area dominated by high porosity carbonates. The effective stress exerted by 1100 m of ooze and chalk corresponds to that exerted by 813 m of siliciclastics in the North Sea, and the velocity–depth gradient consequently becomes $1100/813 = 1.35$ times the gradient of 1 m/s/m observed at ODP Site 807, a value in agreement with the 1.3 m/s/m estimated for the first segment of the revised baseline.

The shift towards higher velocities for the revised baseline results in a reduction in estimates of erosion by up to 210 m, and an increase in estimates of overpressure by up to 2 MPa for data points that plot above and below the line, respectively (overcompaction due to overpressure: $dZ_B/100 = 210/100 \text{ MPa} \approx 2 \text{ MPa}$; see Japsen, 1998). The increased overpressure that the revised model predicts is an improvement relative to the original model which explained only 80% of the observed overpressure in the Chalk for 52 wells located away from diapirs and

where the overpressure exceeded 4 MPa (Japsen, 1998). The corresponding percentage based on the revised baseline is 91%. This improvement is particularly clear for data from relatively shallow depth/moderate overpressure; e.g. the Danish Dan field where overpressure is 7.3 MPa, and for which the overpressure prediction from velocity data has been increased from 4.3 to 6.5 MPa.

References

- Al-Chalabi, M., 1997. Instantaneous slowness versus depth functions. *Geophysics* 62, 270–273.
- Bailey, S.W., 1980. Structure of layer silicates. In: Brindley, G.W., Brown, G. (Eds.), *Crystal Structures of Clay Minerals and Their X-ray Identification*. Mineralogical Society, London, pp. 1–124.
- Bertelsen, F., 1980. Lithostratigraphy and Depositional History of the Danish Triassic. Geological Survey of Denmark, Copenhagen.
- Borre, M., Fabricius, I., 1998. Chemical and mechanical processes during burial diagenesis of chalk: an interpretation based on specific surface data of deep-sea sediments. *Sedimentology* 45, 755–769.
- Bulat, J., Stoker, S.J., 1987. Uplift determination from interval velocity studies, UK, southern North Sea. In: Brooks, J., Glennie, K.W. (Eds.), *Petroleum Geology of North-West Europe*. Graham & Trotman, London, pp. 293–305.
- Cameron, T.D.J., 1993. 4. Triassic, Permian and Pre-Permian of the Central and Northern North Sea. British Geological Survey, Nottingham.
- Cameron, T.D.J., Crosby, A., Balson, P.S., Jeffery, D.H., Lott, G.K., Bulat, J., Harrison, D.J., 1992. United Kingdom Offshore Regional Report: The Geology of the Southern North Sea. British Geological Survey, London.
- Chadwick, R.A., Kirby, G.A., Baily, H.E., 1994. The post-Triassic structural evolution of north-west England and adjacent parts of the East Irish Sea. *Proc. Yorkshire Geol. Soc.* 50, 91–102.
- Chapman, R.E., 1983. *Petroleum Geology*. Elsevier, Amsterdam.
- Cope, M.J., 1986. An interpretation of vitrinite reflectance data from the southern North Sea Basin. In: Brooks, J., Goff, J.C., van Hoorn, B. (Eds.), *Habitat of Palaeozoic Gas in N.W. Europe*. Geological Society, London, pp. 85–98.
- Day, G.A., Cooper, B.A., Andersen, C., Burgers, W.F.J., Rønnevik, H.C., Schoneich, H., 1981. Regional seismic structure maps of the North Sea. In: Hobson, G.D., Illing, L.V. (Eds.), *Petroleum Geology of the Continental Shelf of North-West Europe*. Institute of Petroleum, London, pp. 76–84.
- Evans, D.J., 1997. Estimates of the eroded overburden and the Permian–Quaternary subsidence history of the area west of Orkney. *Scot. J. Geol.* 33, 169–182.
- Gatliff, R.W., Richards, P.C., Smith, K., Graham, C.C., McCormac, M., Smith, N.J.P., Long, D., Cameron, T.D.J., Evans, D.,

- Stevenson, A.G., Bulat, J., Ritchie, J.D., 1994. United Kingdom Offshore Regional Report: The Geology of the Central North Sea. The British Geological Survey, London.
- Glennie, K.W., Boegner, P.L.E., 1981. In: Illing, L.V., Hobson, G.D. (Eds.), *Sole Pit Inversion Tectonics*. Institute of Petroleum, London, pp. 110–120.
- Hansen, S., 1996. Quantification of net uplift and erosion on the Norwegian Shelf south of 66°N from sonic transit times of shale. *Nor. Geol. Tidsskr.* 76, 245–252.
- Heasler, H.P., Kharitonova, N.A., 1996. Analysis of sonic well logs applied to erosion estimates in the Bighorn Basin, Wyoming. *AAPG Bull.* 80, 630–646.
- Hillis, R.R., 1995. Quantification of Tertiary exhumation in the United Kingdom southern North Sea using sonic velocity data. *AAPG Bull.* 79, 130–152.
- Hottmann, C.E., Johnson, R.K., 1965. Estimation of formation pressures from log-derived shale properties. *J. Pet. Technol.* 17, 717–723.
- Jankowsky, W.J., 1962. Diagenese und Ölinhalt als Hilfsmittel für die strukturgeschichtliche Analyse des Nordwestdeutschen Beckens. *Z. Deutschen Geol. Ges.* 114, 452–460.
- Japsen, P., 1993. Influence of lithology and Neogene uplift on seismic velocities in Denmark; implications for depth conversion of maps. *AAPG Bull.* 77, 194–211.
- Japsen, P., 1997. Regional Neogene exhumation of Britain and the western North Sea. *J. Geol. Soc. (London)* 154, 239–247.
- Japsen, P., 1998. Regional velocity–depth anomalies, North Sea Chalk: a record of overpressure and Neogene uplift and erosion. *AAPG Bull.* 82, 2031–2074.
- Japsen, P., 1999. Overpressured Cenozoic shale mapped from velocity anomalies relative to a baseline for marine shale, North Sea. *Pet. Geosci.* 5, 321–336.
- Jeanes, C.V., 1995. Clay mineral stratigraphy in Palaeozoic and Mesozoic red bed facies onshore and offshore UK. In: Dunay, R.E., Hailwood, E.A. (Eds.), *Non-Biostratigraphical Methods of Dating and Correlation*. Geological Society, London, pp. 31–55.
- John, H., 1975. Hebung- und Senkungsvorgänge in Nordwestdeutschland. *Erdoel Kohle* 28, 273–277.
- Johnson, H., Warrington, G., Stoker, S.J., 1994. 6. Permian and Triassic of the Southern North Sea. British Geological Survey, Nottingham.
- Lindgreen, H., 1991. Elemental and structural changes in illite/smectite mixed-layer clay minerals during diagenesis in Kimmeridgian–Volgian (–Ryazanian) clays in the Central Trough, North Sea and the Norwegian–Danish Basin. *Bull. Geol. Soc. Den.* 39, 1–82.
- Marie, J.P.P., 1975. Rotliegendes stratigraphy and diagenesis. In: Woodland, A.W. (Ed.), *Petroleum and the Continental Shelf of North-West Europe*. Applied Science Publ., London, pp. 205–211.
- Michelsen, O., 1989. Revision of the Jurassic Lithostratigraphy of the Danish Subbasin. Geological Survey of Denmark, Copenhagen.
- Nielsen, L.H., Japsen, P., 1991. Deep Wells in Denmark, 1935–1990; Lithostratigraphic Subdivision. Geological Survey of Denmark, Copenhagen.
- Pedersen, G.K., 1985. Thin, fine-grained storm layers in a muddy shelf sequence: an example from the Lower Jurassic in the Stenlille 1 well, Denmark. *J. Geol. Soc. (London)* 142, 357–374.
- Riis, F., Jensen, L.N., 1992. Introduction; measuring uplift and erosion; proposal for a terminology. *Nor. Geol. Tidsskr.* 72, 223–228.
- Scherbaum, F., 1982. Seismic velocities in sedimentary rocks; indicators of subsidence and uplift. *Geol. Rundsch.* 71, 519–536.
- Schmidt, B.J., 1985. Clay mineral investigation of the Rhaetic–Jurassic–Lower Cretaceous sediments of the Børglum 1 and Uglev 1 wells, Denmark. *Bull. Geol. Soc. Den.* 34, 97–110.
- Urmos, J., Wilkens, R.H., Bassinot, F., Lyle, M., Marsters, J.C., Mayer, L.A., Mosher, D.C., 1993. Laboratory and well-log velocity and density measurements from the Ontong Java Plateau: new in-situ corrections to laboratory data for pelagic carbonates. In: Berger, W.H., Kroenke, L.W., Mayer, L.A., Janacek, T.R. (Eds.), *Proceedings of the Ocean Drilling Program. Scientific Results. Ocean Drilling Program, College Station, TX*, pp. 607–622.
- van Hoorn, B., 1987. Structural evolution, timing and tectonic style of the Sole Pit inversion. *Tectonophysics* 137, 239–284.
- van Olphen, H., 1966. Collapse of potassium montmorillonite clays upon heating — “potassium fixation”. In: Bailey, S.W. (Ed.), *Clays and Clay Mineralogy*. Pergamon, New York, pp. 393–405.